Solar and interplanetary sources of major geomagnetic storms during 1996–2002

Nandita Srivastava and P. Venkatakrishnan

Udaipur Solar Observatory, Physical Research Laboratory, Udaipur, India

[1] During the 7-year period of the current solar cycle, 64 geoeffective coronal mass ejections (CMEs) were found to produce major geomagnetic storms ($D_{ST} < -100$ nT) at the Earth. In this paper we examine solar and interplanetary properties of these geoeffective coronal mass ejections (CMEs). The observations reveal that full-halo CMEs are potential sources of intense geomagnetic activity at the Earth. However, not all full-halo CMEs give rise to major geomagnetic storms, which complicates the task of space weather forecasting. We examine solar origins of the geoeffective CMEs and their interplanetary effects, namely, solar wind speed, interplanetary shocks, and the southward component of the interplanetary magnetic field, in order to investigate the relationship between the solar and interplanetary parameters. In particular, the present study aims at ascertaining solar parameters that govern important interplanetary parameters responsible for producing major geomagnetic storms. Our investigation shows that fast full-halo CMEs associated with strong flares and originating from a favorable location, i.e., close to the central meridian and low and middle latitudes, are the most potential candidates for producing strong ram pressure at the Earth's magnetosphere and hence intense geomagnetic storms. The results also show that the intensity of geomagnetic storms depends most strongly on the southward component of the interplanetary magnetic field, followed by the initial speed of the CME and the ram pressure.   *INDEX TERMS:* 7513 Solar Physics, Astrophysics, and Astronomy: Coronal mass ejections; 2784 Magnetospheric Physics: Solar wind/magnetosphere interactions; 2788 Magnetospheric Physics: Storms and substorms; 2139 Interplanetary Physics: Interplanetary shocks; *KEYWORDS:* CME, halo CMEs, IP shocks, solar wind, geomagnetic storms, D_{ST} index

1. Introduction

[2] Geomagnetic activity observed at the Earth is generally attributed to the (1) occurrence of CMEs on the Sun and the associated interplanetary shock waves or (2) corotating interaction regions (CIR) produced by high-speed solar wind streams in the interplanetary medium [*Gosling*, 1993a, 1993b; *Bothmer and Schwenn*, 1995; *Luhmann*, 1997; *Crooker and McAllister*, 1997]. CMEs are large expulsions of mass from the Sun and are generally associated with solar prominences or flares. Once launched from the Sun, CMEs travel through the interplanetary medium and, if directed toward the Earth, reach the Earth in 1–4 days depending on their speed. Therefore in order to predict geoeffectiveness of CMEs, one needs to examine the solar data from near the surface of the Sun and follow them through to the Earth. This requires an examination of ground-based and space-based multi-instrument data sets. This is now possible with the advent of the Solar and Heliospheric Observatory (SOHO) [*Domingo et al.*, 1995],

in particular with the Large Angle Spectrometric Coronagraphs (LASCO) aboard SOHO that have capability of imaging the corona from 1.1 to 30 $R_\odot$ [*Brueckner et al.*, 1995] and therefore can be used to track a CME over this range. From the point of view of space weather prediction, fast CMEs (>1000 km s^{-1}) are sources of high energetic particles. Such fast CMEs can give rise to intense geomagnetic storms on arrival at the Earth [*Srivastava and Venkatakrishnan*, 2002]. Although the increase in the number of energetic particles takes place within a few hours of the onset of a CME, the geomagnetic storm generally occurs 1 to 4 days later. It is generally accepted that the initial phase of the resulting geomagnetic storm is triggered by an increase in the plasma pressure accompanied by an increase in the density and speed of the solar wind at and behind the interplanetary shock. The main phase is governed, on the other hand, by the southward component of the interplanetary magnetic field (IMF) [*Burton et al.*, 1975].

[3] In recent years, a number of investigations have been carried out to understand the solar-terrestrial relationship and to ascertain factors that are responsible for severe geomagnetic storms [*Feynman and Gabriel*, 2000; *Plunkett*

et al., 2001; *Wang et al.*, 2002; *Zhang et al.*, 2003]. Several studies of the interplanetary sources of geomagnetic storms show that the increase in the speed of the solar wind and the magnitude of the southward component of the embedded magnetic field are the key interplanetary parameters that determine the geoeffectiveness of a CME [*Cane et al.*, 2000; *Richardson et al.*, 2000]. However, the key solar factors that determine the geoeffectiveness are yet to be clearly identified. There is not enough information as to which characteristics of the solar sources of strong geomagnetic storms influence their interplanetary properties and how. An understanding of such characteristics can help in forecasting the occurrence of strong geomagnetic storms early on. In the present study we investigate the solar and interplanetary conditions that were specific to intense storms observed during 1996–2002 in order to understand the relationships between the solar and interplanetary parameters associated with intense geomagnetic storms. We follow *Tsurutani et al.* [1988] in defining an intense storm as the one whose D_{ST} index is less than −100 nT and is associated with interplanetary structures involving large-intensity ($B_T > 10$ nT) and long-duration (T > 3 hours) negative values of B_z. Here, B_T and B_z refer to the total IMF and southward component of the IMF measured in situ, respectively, and the D_{ST} (Disturbance Storm-Time Index) is a measure of the change in global high-altitude equatorial ring current and is determined from the variation of the Earth's horizontal magnetic field. We further classify the storms as superintense ($D_{ST} < -200$ nT) and intense (-200 nT $< D_{ST} < -100$ nT) [cf. *Gonzalez et al.*, 1999].

2. Observational Data Sets

[4] The data sets used in this study include all the 64 geoeffective CMEs that occurred between 1996 and 2002 and gave rise to intense geomagnetic storms (D_{ST} index < −100 nT). We used LASCO and EIT (Extreme Ultraviolet Telescope) [*Delaboudiniere et al.*, 1995] data for studying the solar origins of the CMEs. The EIT produces images of the Sun in four bands including one at 195 Å. The LASCO coronagraphs C2 and C3 images, which give a combined field of view from 2 to 30 $R_\odot$, were used for tracking the CMEs in the outer corona. It is generally agreed that most geoeffective CMEs originate on the front side of the Sun and head toward the Earth [*Howard et al.*, 1982]. They are observed in LASCO images as full halos (360°) or partial halos (>140°). The definition of full or partial halo is based on the azimuthal extent of CMEs in the LASCO field of view [*Webb et al.*, 2000]. The other data sets used include Charge, Element, Isotope, and Analysis System (CELIAS aboard SOHO) data and Advanced Charge Explorer (ACE) data for studying the near-Earth effects of CME passage on the interplanetary medium [*Hovestadt et al.*, 1995; *Stone et al.*, 1998]. The CELIAS instrument aboard SOHO provides in situ measurements of the plasma, i.e., solar wind, density, and temperature. The total magnetic field and the southward component of the interplanetary magnetic field (IMF) values, which are important for understanding the development of intense storms, were obtained from the ACE data archive. The values of D_{ST} indices were obtained from the geomagnetic activity web page of the World Data Center, Japan (available at http://swdcwww.kugi.kyoto-u.ac.jp).

[5] In order to determine the solar source of a geomagnetic storm, we follow a criterion similar to that of *Wang et al.* [2002] and *Zhang et al.* [2003]. We selected a temporal window of 1–5 days before the occurrence of the storm. We looked for a front-side halo in this time window, which originated in a location where significant activity was seen in EIT images. For example, flare, waves, dimming, and arcade formation are some of the features that indicate the launch of a CME in EIT images. If there were near-simultaneous CMEs, the heliocentric location of the activity in EIT images were compared with the position angle of the CMEs to identify the source CME. The time of the first brightening seen in the EIT images (also reported in the halo-mail archive available at ftp://ares.nrl.navy.mil/pub/lasco/halo) was considered the time of initiation of flare/CME activity. The time period between the launch of a CME (as seen in EIT images) and the time of the commencement of the geomagnetic storm at the Earth was considered the transit time of the CME. The time of the commencement of a geomagnetic storm is defined as the time at which the D_{ST} index starts decreasing.

3. Characteristics of Solar Sources of Geomagnetic Storms

3.1. Association With Halos

[6] We found a 100% association of superintense storms with full halos (excess brightness is seen all around the occulter of the LASCO coronagraphs). In other words, the sources of all the superintense storms ($D_{ST} < -200$ nT) could be identified as full halo CMEs for which the angular extent of the emission was approximately 360°. Among the intense storms (-200 nT $< D_{ST} < -100$ nT), ~58% were associated with full halos, while ~25% were associated with partial halos (emission seen in an angular span of greater than 140° in LASCO images). For the remaining 17%, either the LASCO data was not available or the locations of the sources were too close to the limb, and thus neither a full nor a partial halo could be observed. The latter category includes the limb CME of 4 April 2000, which was associated with neither a full nor a partial halo. This study clearly shows that a large majority of the geoeffective events are associated with full or partial halos whose intensity is much above the sensitivity of the coronagraphs so that they could be easily detected in LASCO images. Because all of the superintense/intense storms had their origin in some solar activity on the front side of the Sun and are associated with front-side full or partial halos, it can be hypothesized that the back-side halos are unlikely to give rise to superintense/intense storms.

3.2. Variation in Geoeffectiveness During the Current Solar Cycle

[7] It is important to identify the solar drivers of the geomagnetic activity in order to be able to predict the occurrence of a strong geomagnetic storm. Several workers, for example, *Gosling et al.* [1991], *Tsurutani and Gonzalez* [1997], and *Richardson et al.* [2001], have discussed this aspect in much detail over various periods of the solar activity cycle. On the basis of these studies, one expects a large number of intense geomagnetic storms (-200 nT $< D_{ST} < -100$ nT), close to the solar maximum than during
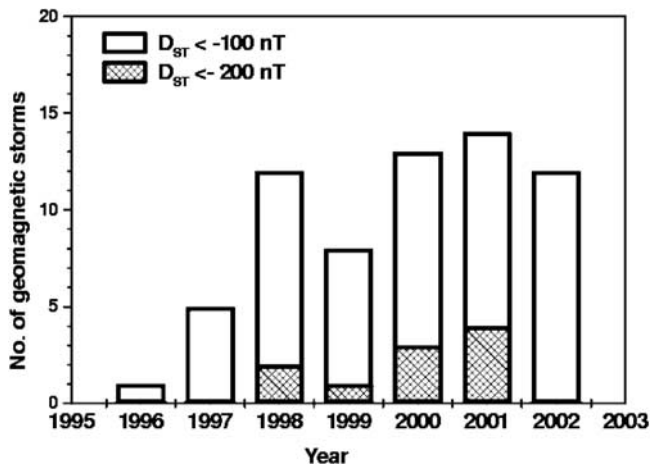
Figure 1. Variation in the number of the geomagnetic storms ($D_{ST} < -100$ nT) with the solar cycle. The filled region denotes the number of superintense geomagnetic storms each year, for the period 1996–2002.

the solar minimum [*Richardson et al.*, 2002]. We extended the period of study made by *Richardson et al.* [2000], who studied the geoeffective events during 1997–2000 to 2003. From our study we found the following. During this period a total of 65 intense geomagnetic storms were recorded (Figure 1). In 1996, i.e., during solar minimum, only one geomagnetic storm was recorded as against 14 geomagnetic storms close to the solar maximum in 2001. However, the only intense geomagnetic storm of the year 1996 which occurred on 23 October 1996 ($D_{ST} \sim -105$ nT) was not related to a CME but due to a CIR feature [*Zhang et al.*, 2003]. We have therefore eliminated this geomagnetic storm from our study for solar sources. The study is thus confined to investigation of solar sources of the remaining 64 geomagnetic storms. During the study period, the number of intense geomagnetic storms increased from five

in 1997 to 13 in 2000, thereby showing an increase with the progress of the solar activity cycle. A significant decline in the number of geomagnetic storms is observed from 1998 to 1999, from 12 to eight events. Further, out of a total of 10 superintense storms ($D_{ST} < -200$ nT) which occurred during 1996–2002 (shown by filled region in Figure 1), the maximum number (four) occurred in the year 2001. The year 1999 is conspicuous because of a decline in the overall number of geomagnetic storms including the superintense events. This decline is consistent with the overall decline in the solar activity and related interplanetary activity in 1999 [*Cane et al.*, 2000]. The observed temporary decline in the number of geomagnetic storms has been attributed to the restructuring of the near-ecliptic solar wind [*Richardson et al.*, 2002].

[8] The average rate of occurrence of intense geomagnetic storms calculated over the period of study, i.e., 1996–2002, is found to be slightly greater than one per month near solar maximum year in 2000. This is almost twice the rate observed in the ascending phase in 1997. In contrast, the average rate of occurrence of CMEs increases by a factor of 10 from solar minimum to maximum. This is evidenced by the fact that during solar minimum the rate of CME occurrence was ~0.3 CME per day while the solar maximum witnessed an average of three CMEs per day [*St. Cyr et al.*, 2000]. This implies that the average rate of intense geomagnetic storms from solar minimum year to solar maximum year increases by a factor of 2, while the number of CMEs increases by a factor of 10. The distinct variation in the rate of all CMEs, and those that are directed earthward, suggests that the conditions that give rise to geomagnetic storms do not depend solely on the phase of the solar cycle. This also follows from a comparative examination of the daily average sunspot numbers obtained from the National Geographical Data Center (NGDC) for this study period (Figure 2) with the number of geomagnetic storms. While the maximum number of observed sunspots steadily increased from 10 in 1996 (solar minimum) to 170 in the year 2001 (solar maximum), the number decreased to
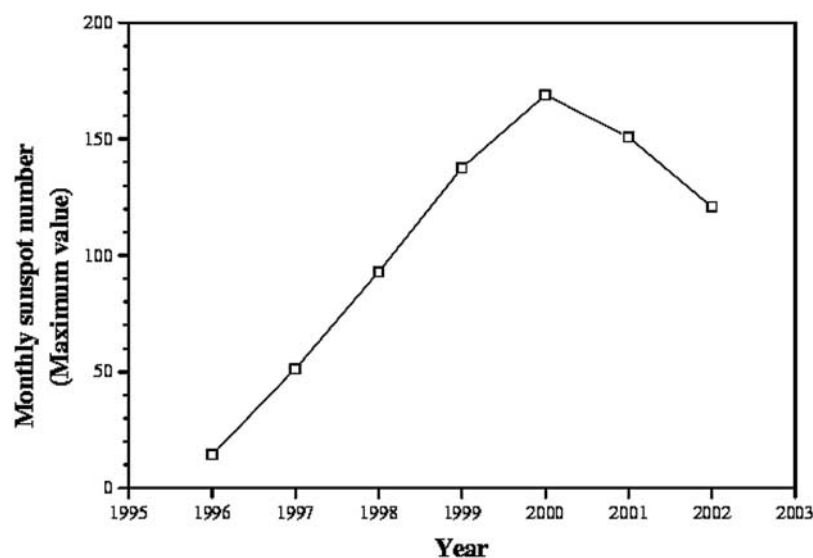

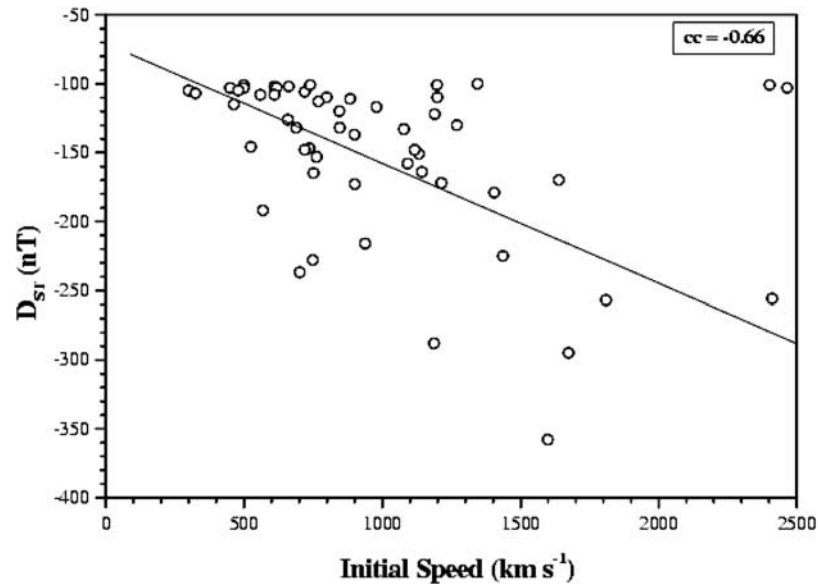**Figure 2.** Sunspot number variation with the solar cycle.

Figure 3. The geomagnetic storm intensity plotted against the initial speeds of CMEs shows a good association.

100 in the year 2002 (descending phase of the solar cycle). If the rate of occurrence of geoeffective CMEs follows the solar cycle, one would expect a rise and fall in the number of geoeffective CMEs by the same factor as that observed in case of the sunspot numbers. However, the lack of correlation between the two (Figures 1 and 2) indicates that other factors (for example, the presence of the corotating interaction regions or CIRs) may also be responsible for more geoeffective CMEs during minimum. It has been shown in the past that CIRs generally contribute to minor and moderate geomagnetic storms [*Lindsay et al.*, 1995]; they can occasionally contribute to strong storms too. In fact, a dual peak has been reported earlier in storm activity near solar maximum [*Gonzalez et al.*, 1990]. The first peak close to the solar maximum arises due to the increased rate of CME related storms, while the second peak occurs around 2 years after the solar maximum and is caused by the corotating streams [*Richardson et al.*, 2000].

3.3. Initial Speeds of the Geoeffective CMEs

[9] The radial speed of earthward halo CMEs cannot be measured directly because of the unfavorable location of the observer at the Earth. Recent observations of the LASCO indicate that CMEs show some distinct characteristics irrespective of their directions. One such characteristic is that the geometrical shape of the ejected material is maintained throughout the field of view of the LASCO coronagraphs [*Webb et al.*, 1997]. Moreover, the angular extent of the interplanetary clouds is comparable to that of the CME close to the Sun, which implies that the angular width of a CME remains constant [*Webb and Jackson*, 1990]. This further implies that the radial propagation is proportional to the lateral expansion of the clouds. Therefore the radial speed of the halo CMEs can be inferred from their lateral expansion speeds. From LASCO images, one can estimate the propagation speed up to 30 $R_\odot$. Beyond this distance, the near-Earth in situ measurements can be used for

determining the speeds of the ejecta. Assuming a uniform expansion of the CME in all the directions, we took the expansion speeds of the halos as a proxy for the radial speed of the halos in order to estimate the probable travel time toward the Earth. With the exception of 10 cases, the initial speeds of all geoeffective CMEs observed during 1996–2002 range between 500 and 2000 km s^{-1}, as observed in the LASCO-C2 field of view. We found a negative Pearson's correlation coefficient of $\sim$0.66 between the initial speed of the CMEs and the geomagnetic activity (Figure 3) at 0.01 significance level (99% confidence level).

[10] In determining the correlation coefficient, the CME of 18 April 2001, which had high initial speed $\sim$2400 km s^{-1} and resulted in intense geomagnetic storm ($D_{ST} \sim -103$ nT), has not been included. The fact that this was a limb CME justified its exclusion. Assuming that a CME propagates in straight radial direction, the actual earthward directed speed in this case will be much smaller than the projected speed against the sky plane. Another exceptional case is the CME of 24 September 2001, which started off with a very high initial speed i.e., 2400 km s^{-1}, and produced a geomagnetic storm with relatively lesser magnitude ($D_{ST} \sim -102$) nT. Although the CME originated close to the central meridian, the core of the CME was directed at position angle 105°, and therefore the Earth missed the front of the shock and ejecta and hence the magnitude of the storm was lower compared with what it could have produced if it was directed straight toward the Earth.

[11] Our result is consistent with that of *Srivastava and Venkatakrishnan* [2002], who reported a higher value of correlation coefficient of $\sim$0.83 between the speeds of geoeffective CMEs associated with the intense X-class flares and the strength of the resulting geomagnetic storm. The lower correlation coefficient obtained in the present study can be explained by (1) the fact that *Srivastava and Venkatakrishnan* [2002] used only those CMEs that were
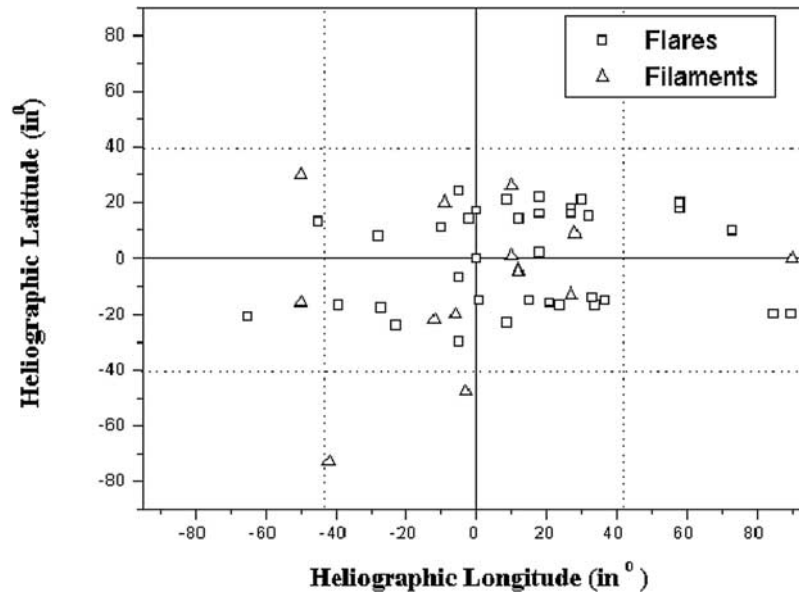
Figure 4. The location of the solar sources of the geoeffective events during 1996–2002. The sources have been denoted by a square/triangle if the CME is associated with a flare/filament, respectively.

associated with X-class events, which are generally known to have a higher speed range as compared to CMEs associated with low X-ray flux, i.e., B, C, and M class events; (2) the assumption that the halo speeds are constant in all directions may not be true; (3) the assumption that the radial speeds of the halo CMEs are the same as their lateral expansion speeds may not be exactly correct, thus contributing to some errors in the estimation of the initial speeds. Nevertheless, the correlation coefficient of 0.66 between the initial speeds of the geoeffective CMEs and the strengths of the resulting geomagnetic storms indicates that the initial speed could be used as one of the parameters for predicting geomagnetic activity [cf. *Cane et al.*, 2000; *Gopalswamy et al.*, 2000]. Measurements of the CME speeds show that a large percentage of the geoeffective CMEs (62%) have initial speeds higher than 700 km s^{-1}, which is even higher than the typical high speed solar wind. For 9% of the events the initial speeds could not be measured because of either data gaps in LASCO observations or because the SOHO spacecraft went into nonfunctional mode. We also found that there are a few slow CMEs, particularly during solar minimum, which proved to be geoeffective. Such events appear to be an exception to the results obtained by *Gosling et al.* [1990] and *Gonzalez et al.* [1998] that only fast CMEs can produce severe geomagnetic storms.

3.4. Location of Solar Sources

[12] The location of the origin of halo CMEs seems to be crucial for their impact on the Earth. A few earlier studies have shown that all front-side halos may be geoeffective provided that they arise from favorable locations, i.e., they originate close to the central meridian and at low latitudes. [*Gonzalez et al.*, 1996; *Srivastava et al.*, 1997, 1998; *Srivastava and Venkatakrishnan*, 2002; *Wang et al.*, 2002; *Zhang et al.*, 2003]. In the present study we find a far less pronounced longitudinal asymmetry in the distribution of source region of the geoeffective CMEs. Almost 47% of

them appear from the east of the central meridian, and 53% appear from the west side. This asymmetry is much smaller compared with that reported by *Wang et al.* [2002] and *Zhang et al.* [2003]. Our results based on 7 years data are in better agreement with those of *Cane et al.* [2000], who report a symmetrical longitudinal distribution of the locations of the origins of the geoeffective CMEs.

[13] From an examination of the origins of all the geoeffective CMEs, it was found that the location of the CMEs is important as most of geoeffective CMEs have their origins near the central meridian and at low and middle latitudes with 12 exceptions (Figure 4). The majority of the events originated within ±40° of the central meridian and ±40° of the equator. There appears to be no hemispherical preference in halo CMEs that reach the Earth, as reported by *Cane et al.* [2000] and *Wang et al.* [2002]. In our investigation, we find 33 events originated in the northern hemisphere as against 31 events in the southern hemisphere. CMEs in general show larger variation in latitude with the solar activity cycle extending up to the poles, as compared with the active regions, which are confined to moderate latitudes [*Hundhausen*, 1997]. Our analysis shows that the geoeffective CMEs are generally confined to the active region belt, i.e., low and moderate latitudes.

3.5. Prediction of Arrival Time of Geoeffective CMEs

[14] The travel time or the arrival time of the geoeffective CMEs is an essential parameter in space weather prediction. The travel time of a CME is defined as the difference in the start time of the CME as observed in EIT images and the start time of the geomagnetic storm at the Earth. The time of the start of flare/CME activity in EIT images has been taken as the time of the first brightening/activity seen in the EIT images, reported in the halo-mail archive (available at ftp:// ares.nrl.navy.mil/pub/lasco/halo). As the normal cadence of recording EIT images is ~12 min, a maximum error of ~12 min can occur in calculating the time of flare/CME.
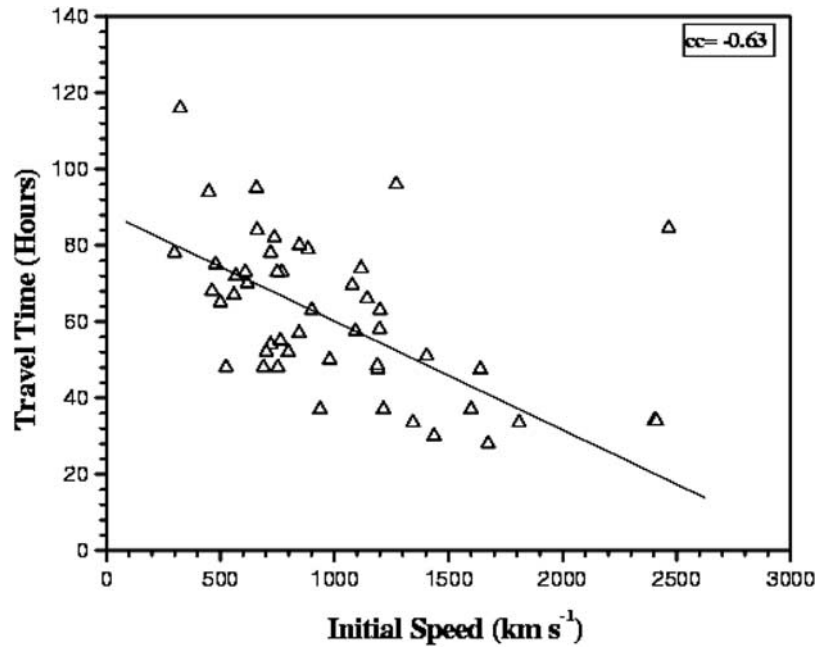
Figure 5. The dependence of the arrival time of the geoeffective events at the Earth on their initial speeds as measured by LASCO coronagraph.

Once the timing of the launch of the CME is known, the uncertainty in the prediction of the arrival time of the CMEs at the Earth is of the order of a few hours only. However, the lack of observations in the region between the near-Sun and near-Earth leads to the poor prediction of the arrival time. *Brueckner et al.* [1998] found that the travel time for most of the CMEs during solar minimum is almost 80 hours. In our data set the minimum and maximum transit time recorded was 28 and 120 hours, respectively, as compared with 34 (minimum) and 135 (maximum) hours transit time found by *Zhang et al.* [2003]. This may be due to the different definitions of the transit time of the CME adopted by different authors; our definition of the CME arrival time/transit time is the difference in the timings of the start of the CME and the time of the onset of the geomagnetic storm marked by the decrease in D_{ST} values. *Zhang et al.* [2003] calculated two different transit times, (1) transit time from solar CME-ICME arrival and (2) solar CME-D_{ST} peak time. On the other hand, *Wang et al.* [2002] defined the same as the difference in the timings of the start of the CME and the time of the peak in D_{ST} values. The present study indicates that the arrival time shows a strong dependence on the initial speeds of the CMEs (Figure 5). In particular, the CMEs with high speeds >1500 km s^{-1} arrive in less than 40 hours. An exception is the event of 18 April 2001, which started off with a speed of 2465 km s^{-1} and arrived at the Earth in 85 hours. This particular case is exceptional as it occurred at the west limb and hence was only partially directed toward the Earth. For initial speeds ranging between 1000 and 1500 km s^{-1}, the travel time ranges between 50 and 70 hours, with a few exceptions. For the CMEs with initial speeds ranging between 500 and 1000 km s^{-1}, the arrival time ranges between 45–85 hours.

[15] A number of attempts have been made in recent years to predict the arrival time of CMEs at the Earth, for example, by *Cane et al.* [2000] and *Gopalswamy et al.* [2000, 2001a,

2001b]. *Gopalswamy et al.* [2000] proposed an empirical model to predict the arrival time of the CME. They also considered the acceleration of the CMEs, taking into account the effects of projection, to predict the occurrence of geomagnetic storms. It may be pointed out that our definition is very different from that adopted by *Gopalswamy et al.* [2000], who estimated the arrival time of ICMEs using magnetic signatures, and *Cane et al.* [2000], who used cosmic ray depression to estimate the arrival time. Therefore a direct comparison of our results with those of *Gopalswamy et al.* [2000] and *Cane et al.* [2000] cannot be made. Our analysis shows a Pearson's correlation coefficient of −0.63 between the arrival time of geoeffective CMEs and the initial speeds of the CMEs at 0.01 significance level. This result is consistent with the results of *Wang et al.* [2002], obtained from their study of 15 events that were associated with severe storms ($K_p > 5$). *Zhang et al.* [2003] showed that the arrival time can be best predicted by the formula

$$T = 96 - V/21, \tag{1}$$

where T is the arrival time in hours and V is the initial speed of the CME in km s^{-1}. On the basis of their analysis of geoeffective events during 1997–2000, *Wang et al.* [2002] determined an empirical relation for the arrival time, given by

$$T = 27.98 + \left[(2.11 \times 10^4)/V\right], \tag{2}$$

where T and V are the same as defined above. From the regression analysis of the 64 events observed during 1996–2002 studied in this paper, we found the following relation between the transit time and the initial speed,

$$T = 86.9 - 0.026V. \tag{3}$$

While *Zhang et al.* [2003] and the present study shows a dependence of T on the initial velocity, V, *Wang et al.* [2002] found a 1/V variation, the difference arising due to different functional fits considered for the data set. In the present study and that by *Zhang et al.* [2003], a linear relationship between V and T was considered, while *Wang et al.* [2002] fitted a nonlinear function to the data. However, as there is some uncertainty involved in both the measurements, i.e., in the velocity because of the projections effects and also in the estimation of the arrival time, we believe it is only reasonable to assume a simple empirical formula based on a linear relation than a nonlinear or quadratic fit. A linear regression coefficient of -0.63 between initial speed and the arrival time suggests that this assumption is not invalid. Our empirical relation holds good for estimating the transit time of a majority of geoeffective CMEs. However, it may not be applicable for very slow ones.

3.6. Association With Other Solar Activity: EIT Waves and LDE Phenomena

[16] A statistical investigation of the solar sources of the geoeffective CMEs reveals that 75% of the CMEs were associated with flares, whereas 25% of the CMEs were associated with the eruptive filaments. This is in agreement with the ratio of association of flares to eruptive prominences, namely 70% to 30% for the sources of the geoeffective CMEs [*Webb*, 1992]. This result also implies that flares are more important from the point of view of space weather prediction, which is in agreement with the findings of *Wang et al.* [2002]. However, the strength of the related geomagnetic storm does not appear to have a relation with the magnitude of the flare [cf. *Srivastava and Venkatakrishnan*, 2002; *Zhang et al.*, 2003]. We also examined the daily mpeg movies of all the events obtained by the EIT aboard SOHO (available at http://star.mpae.gwdg.de/daily_mpg) and found that 26 events were accompanied with EIT waves (available at http://lasco-www.nrl.navy.mil/halocme.html). *Thompson et al.* [1998] studied these waves and found them to be a fast-mode MHD disturbance, which propagate radially outward in all directions with initial speed of $250-400$ km s^{-1} before they are observed as halos in the coronagraph field of view. Furthermore, $\sim$74% of the flare-associated geoeffective CMEs in our period of study were also accompanied by EIT waves. This is a significant percentage. Thus the presence of EIT waves is possibly an important signature of geoeffective CMEs, particularly the major ones.

[17] The association of EIT waves with a geoeffective CME can give a clue on the nature of the propagation of the CME in the initial phase, i.e., close to the Sun. On the basis of the assumption that the EIT waves are the signatures of MHD waves [*Thompson et al.*, 1998], it is possible to hypothesize that these MHD waves are the manifestations of the restructuring of coronal magnetic field lines. Owing to the low plasma beta in the corona, the restructuring of the field lines forces the plasma to move about with alfvenic speeds, which are supersonic. Such supersonic motions result in shocks that directly input mechanical energy into the corona at a rate that is faster than the rate of dynamical relaxation of the solar wind. This kind of rapid energy input may result in a blast wave. A CME might well be the result of such a blast wave. *Venkatakrishnan and Ravindra* [2003]

have found that the expansion velocity of CMEs varies as the 0.26th power of the magnetic potential energy of the associated magnetic region. This dependence closely resembles the 1/5th power law dependence of the expansion velocity on the energy of the blast in the classical Sedov solution.

[18] Another much discussed signature of a geoeffective CME is an increase in X-ray emission flux which is also known as long duration event or LDE [*Sheeley et al.*, 1975; *Kahler*, 1977; *Webb and Hundhausen*, 1987]. We found four LDE cases of duration greater than 6 hours which were classified as superintense events. Moreover, there were moderate LDEs of $3-5$ hours duration associated with the other 22 cases of geoeffective events studied in this paper. We found that the LDE phenomenon is observed for only $\sim$50% of the geoeffective events and thus the association of an LDE cannot be considered as a significant predictor of a geoeffective CME.

4. Characteristics of Interplanetary Sources of Major Storms

[19] Our statistical investigation of the solar sources of the intense and superintense geomagnetic storms that occurred during $1996-2002$ reveals that fast halo CMEs that are associated with flares and originate in central and midlatitudes of the Sun can possibly be used for predicting intense geomagnetic activity with some degree of confidence. This is in agreement with some of the earlier works done by *Tsurutani et al.* [1990] and *Shea and Smart* [1996]. The investigation further indicates that none of the other solar sources can be used as a significant predictor in space weather forecasting. However, for predicting the magnitude and the onset time of geomagnetic storms, it is also important to understand the interplanetary consequences of geoeffective CMEs. It is therefore necessary to identify key factors that govern the propagation of a CME in the interplanetary medium and crucial parameters of interplanetary CMEs that are responsible for the development of severe geomagnetic storms. Several studies have been undertaken in the recent past to understand the interplanetary causes of major storms such as those by *Kamide et al.* [1998], *Gonzalez et al.* [1999], and *Feynman and Gabriel* [2000, and references therein]. The contributions of the various components of the solar wind, namely, ICMEs, shocks, etc., to the geomagnetic activity has also been studied in details for three solar cycles $(1972-2000)$ by *Richardson et al.* [2002].

[20] In the following section we discuss the characteristics of the interplanetary sources of major storms that occurred during $1996-2002$. We attempt to relate these characteristics to their solar origins.

4.1. Solar Wind and Interplanetary (IP) Shock Properties

[21] The main cause of intense geomagnetic storms is believed to be large interplanetary (IP) structures which have an intense, long-duration, and southward B$_z$ [*Gonzalez et al.*, 1999]. They interact with the Earth's magnetic field and facilitate the transport of energy into the Earth's atmosphere through the reconnection process. However, the geoeffectiveness of CMEs, or the strength of the resulting storms,

Table 1. Statistics for the Period of January 1996 to December 2002[a]

Storm Intensity	IP Shocks Association	Number of Events	D_{ST}	K_p
Superintense	100%	10	$D_{ST} < -200$	$7 < K_p < 9$
Intense	61%	54	$-200 < D_{ST} < -100$	$5 < K_p < 7$

[a]Total number of events is 64.

depends upon whether the magnetosphere is hit by (1) an interplanetary CME or ICME accompanied by an IP shock or (2) by shock only [*Gosling et al.*, 1991]. Table 1 gives the statistics for the 64 geoeffective events recorded during 1996–2002. The table shows that all superintense ($D_{ST} < -200$ nT) storms are associated with the IP shocks or with fast ejecta, while 61% of the intense storms (-200 nT $< D_{ST} < -100$ nT) are associated with IP shocks. This suggests that intense storms are not always caused by strong shocks.

[22] In the present study we focus on the IP properties of CMEs that led to intense and superintense geomagnetic storms. Strong interplanetary shocks are characterized by a sharp rise in the solar wind speed and density. This leads to an increase in ram pressure, which is responsible for the sudden compression of the Earth's magnetosphere. The ram pressure is proportional to nV^2, where n is the proton density and V is the solar wind speed and is a measure of the impact of an IP shock and ejecta on the magnetosphere. The local in situ shock speed was calculated using the solar wind data recorded by the CELIAS and substituting in the Rankine-Hugoniot conservation relation [*Hundhausen*, 1972], which is as follows

$$V_{sh} = \frac{n_2 v_2 - n_1 v_1}{n_2 - n_1},\qquad(4)$$

where n and v denote the density and flow speed of the solar plasma and the subscripts 1 and 2 represent the preshock and

postshock solar wind properties. The shock speeds estimated in this way range between 360 and 1200 km s^{-1}. A plot of the shock speeds and the D_{ST} index shows a weak correlation of -0.28 (Pearson's correlation coefficient at 99% confidence level) between the two, which implies that the strength of a geomagnetic storm at the Earth depends weakly on the shock speed (Figure 6). Further, it is interesting to note that the shock and transit speeds have a much smaller range of 400–1200 km s^{-1} compared with the initial expansion speeds, which typically lie in the range of 400–2500 km s^{-1} (Figure 7). This implies that a high-speed CME possibly decelerates and slows down during its propagation from the Sun to the Earth. The data suggest a net reduction of ~400 km s^{-1} in the CME speed as it propagates outward in the direction of the Earth. However, because of the large scatter in Figure 7, the above inferences cannot be considered as definitive. Furthermore, a correlation coefficient of 0.40 obtained between the initial speed and the shock speed implies that the value of the shock speed is not dictated by initial speed. We calculated another quantity characterizing the interplanetary sources, namely, the ram pressure which is the pressure exerted by the disturbed solar wind on the Earth's magnetosphere, and is given by the following formula

$$P_r = n_p m_p v_p^2,\qquad(5)$$

where n_p, m_p, and v_p denote the proton density, proton mass, and the velocity of the protons in the solar wind, respectively. The ram pressure value calculated in dynes cm^{-2} for all geoeffective events under study has been plotted versus D_{ST} index in Figure 8. The plot shows a negative Pearson's correlation coefficient (0.64) at 99% confidence level between the two quantities. Because we find a reasonable better correlation between the ram
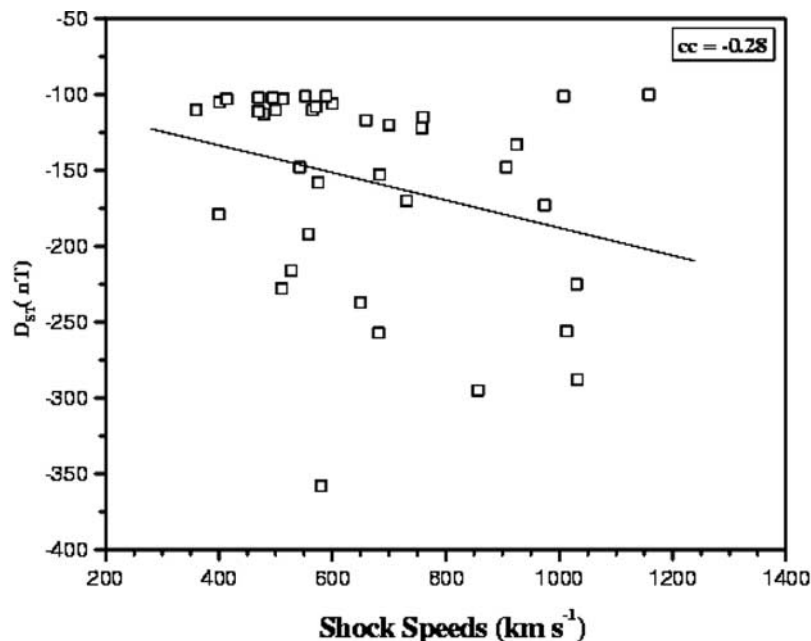

Figure 6. A plot of the magnitude of the geomagnetic storm versus the shock speed shows a poor relation between the two parameters.
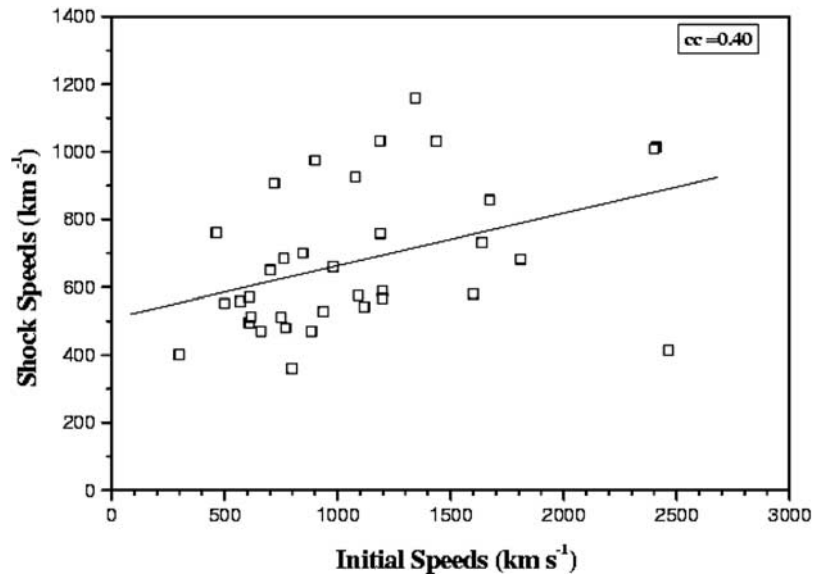
Figure 7. Weak dependence of the shock speed on the initial expansion speed of the associated halo CMEs (correlation coefficient ∼0.4).

pressure (an important parameter for space weather prediction) and the D_{ST} index, it follows that we should investigate the factors that influence this quantity from the point of view of its solar source. The estimation of the ram pressure involves knowledge of the speed (V_p) behind the shock (it varies as V_p^2) and the density. Using the measured values of initial speeds and the solar wind velocity (V_p), one finds a correlation coefficient of 0.58 between the initial speeds and V_p (Figure 9) and 0.62 between initial speeds and V_p^2. If the initial speed is assumed to be the only factor influencing the value of the ram pressure, one may deduce that a similar correlation coefficient should exist between the initial speeds and the ram pressure. However, we obtain a lower correlation coefficient of 0.44 between initial speeds and ram pressure. This implies that the density plays an important role in reducing the correlation. This is confirmed from the plot of initial speeds and the solar wind density in the IP medium as measured by CELIAS, as we find no relation between the two quantities (Figure 10). An outlier data point in this graph corresponds to the solar wind density associated with the CME of 29 March 2001 in AR9393, which led to the strongest
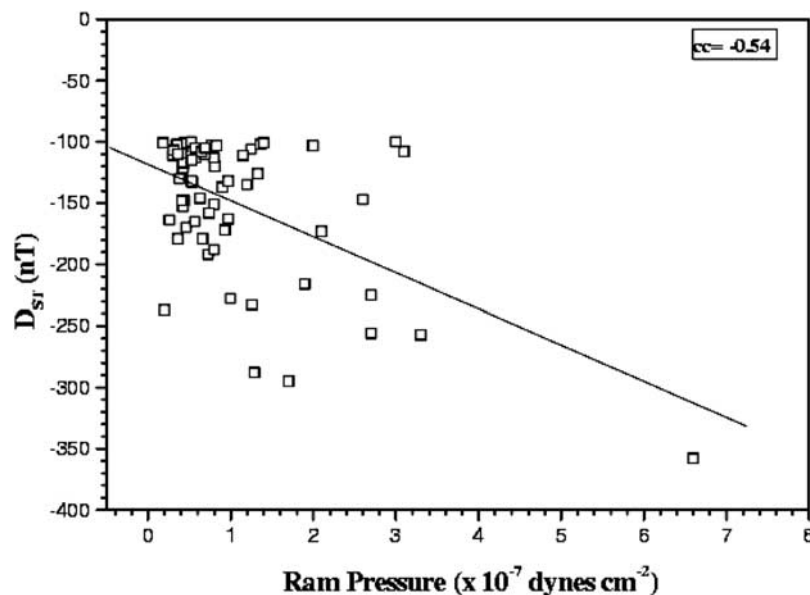

Figure 8. Strong dependence of the ram pressure exerted by the disturbed solar wind on the Earth's magnetosphere and the strength of the related geomagnetic storm.
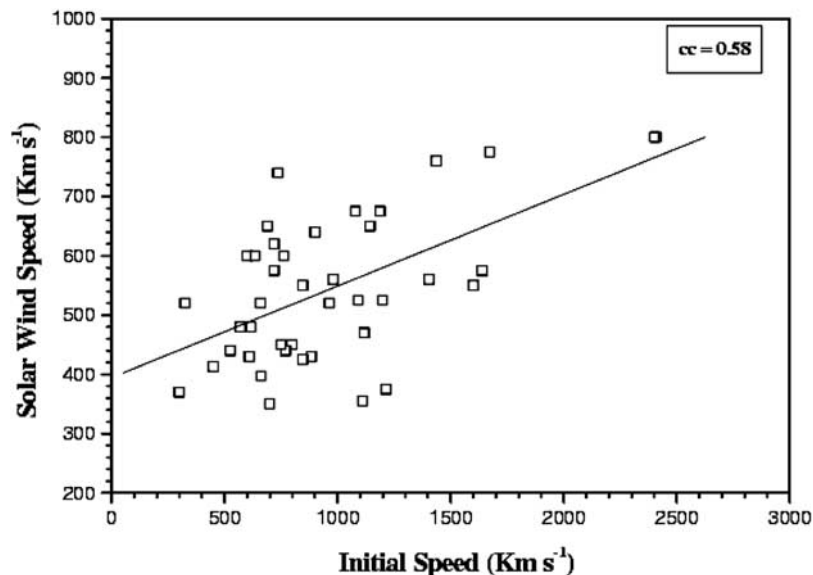
Figure 9. A plot of initial speeds as measured from LASCO and the solar wind speeds measured in situ shows a good relation between the two quantities.

storm ($D_{ST} < -358$ nT) recorded during the period of the study. The lack of any relation between the density of the solar wind and the initial speed also explains the poor correlation coefficient obtained between the shock speeds and the initial speeds since the shock speeds depend on the values of density. In order to predict the strength of the shock, one does require knowledge of the initial speed, which can be measured. For an improved prediction, one not only needs additional information of the initial density of the CME but also the variation in its density as it propagates from the Sun to the Earth.

4.2. Significance of B_z and VB_z in Geomagnetic Activity

[23] Earlier studies suggest that the geoeffectiveness of solar wind depends upon the speed and the embedded southward magnetic field [*Burton et al.*, 1975]. It is the coupling between the solar wind plasma and the magnetic field orientation that defines the magnitude of a geomagnetic storm. We also find a Pearson's correlation coefficient of 0.70 between the D_{ST} values and the maximum southward component of the interplanetary magnetic field, i.e., $|B_z|$ at 99% confidence level. This implies that the configuration of the interplanetary magnetic fields at the time of arrival should be known in order to make accurate predictions of its geoeffectiveness and to avoid the false alarms of magnetic storms. Furthermore, the variation of B_z plays a crucial role in determining the amount of solar wind energy, which is transferred to the magnetosphere [*Gonzalez et al.*, 1989]. In order to investigate the solar wind-magnetosphere coupling mechanism, we also analyzed the correlation between the geomagnetic storm intensity and VB_z, which is helpful in understanding the mechanism for magnetospheric energization of the storms. Figure 11 shows the dependence of the D_{ST} values on the values of $|VB_z|$ (Pearson's cc ~ -0.66 at 99% confidence level). The result is as expected because the D_{ST} index is a measure of the ring current which increases with the increase in the value of the southward component of the magnetic field. The high correlation coefficient between the $|VB_z| - D_{ST}$ and

$|B_z| - D_{ST}$ suggests that $|VB_z|$ and $|B_z|$ both are reliable predictors of the intensity of the geomagnetic storm.

5. Results and Conclusions

[24] The LASCO observations reveal that the total number of the full or partial halos recorded during 1996–2002 is much higher than the number of geomagnetic storms recorded during the same period. This is possibly due to the fact that the ejecta associated with about half of the front-side halo CMEs do not reach the Earth because they do not originate at a favorable location. However, even if the above criterion is met, the strengths of the geomagnetic storm show large variation. The role of the southward component of the interplanetary magnetic field at the time of impact may therefore be crucial. Our investigation of the geoeffective CMEs during 1996–2002 provide crucial information on the estimation of the arrival time of the intense geomagnetic storms within an error of few hours. In order to predict the strength of geomagnetic storms with a better accuracy, one needs to understand completely the factors influencing the storm severity, namely, the initial speed of CMEs and their propagation characteristics in the interplanetary medium. In Table 2 are listed the Pearson's correlation coefficients between the D_{ST} indices and various solar and interplanetary parameters examined in this paper. The table shows that the intensity of geomagnetic storms is strongly related to the quantity B_z, followed by initial speeds and ram pressure of the geoeffective CME.

[25] We conclude the following from our study.

[26] 1. The frequency of occurrence of geoeffective CMEs in solar maximum is almost twice the frequency in solar minimum. On an average, the frequency of geoeffective CMEs is one per month as compared with one every 2 months during solar minimum. Although the rate of occurrence of CMEs increases by a factor of 10 from solar minimum to maximum, the rate of occurrence of intense geoeffective CMEs only doubles. This implies that only a small percentage of all mass ejections are directed earth-
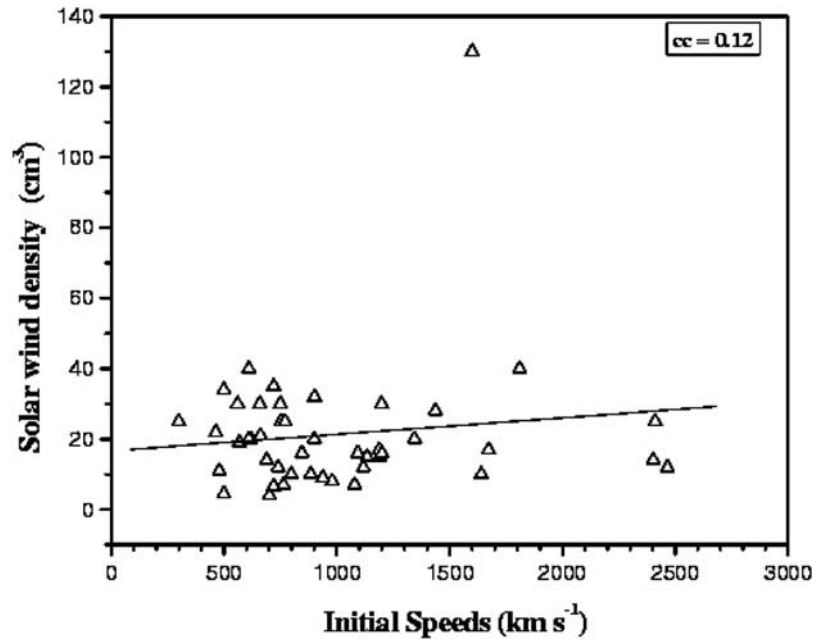
Figure 10. A plot of initial speeds of the CMEs and the solar wind density measured in situ behind the shock shows no relation between the two quantities.

ward and out of these only a few succeed in producing intense geomagnetic activity at the Earth.

[27] 2. The location of the origin of CMEs is important in predicting whether or not it will be geoeffective. The area between ±40° in longitude and ±40° in latitude appears to be particularly favorable for ensuring a good link for the Sun-Earth connection. Our result is in agreement with earlier results of *Webb et al.* [2000], *Cane et al.* [2000], *Gopalswamy et al.* [2000], and *Wang et al.* [2002]. It also indicates that the criteria do not depend upon the phase of the solar cycle.

[28] 3. A larger number of geoeffective CMEs are associated with flares than with eruptive filaments/prominences,

which implies that flare-associated CMEs are more likely to produce intense magnetic storms. The association of flares is larger during the maximum than during the minimum, which implies a dependence on the phase of the solar cycle. This is consistent with the findings of *Brueckner et al.* [1998] and *Wang et al.* [2002]. We also found that the flare importance does not always play a key role in determining the strength of a storm.

[29] 4. A significant association (74%) of EIT waves with the flare-associated geoeffective CMEs implies that the presence of EIT waves is an important signature of a potentially geoeffective CME. It can provide a clue on the launch mechanism and propagation of a geoeffective CME;
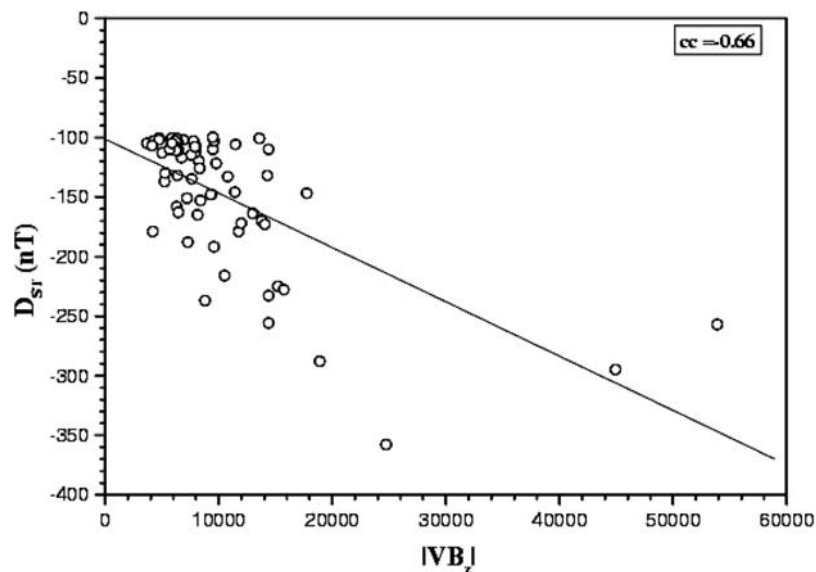

Figure 11. Correlation between $|VB_z|$ and D_{ST} index for the chosen geoeffective events.

Table 2. Pearson's Correlation Coefficients Between the D_{ST} Indices and Various Solar and Interplanetary Parameters

Solar and IP Quantity That Influence the Strength of Storm (D_{ST})	Pearson's Correlation Coefficient at 99% Confidence Level
$D_{ST} - V_i$ (Initial speed)	−0.66
$D_{ST} - V_{SH}$ (Shock velocity)	−0.28
$V_i - V_{SH}$	−0.40
$D_{ST} - P_r$ (Ram pressure)	−0.64
$D_{ST} - B_z$ (Southward directed IMF)	−0.70
$D_{ST} - VB_z$ (Solar wind-magnetospheric coupling parameter)	−0.66
$V_i - V_p$ (Solar wind speed)	0.58
$V_i - P_r$	0.44
$V_i - T$ (Arrival time)	−0.63

however, the speed of the EIT waves, which ranges between 250 and 400 km s^{-1}, does not have any bearing on the geoeffectiveness of a CME.

[30] 5. The initial speed of a CME close to the solar surface as measured in LASCO field of view determines to some extent the strength of the resulting geomagnetic storm. A correlation coefficient value of ∼0.66 between these two quantities indicates that initial speed can be a useful parameter for predicting the occurrence of a strong geomagnetic storm, which reinforces our earlier result [*Srivastava and Venkatakrishnan*, 2002]. The present study indicates that the superintense geomagnetic storms ($D_{ST} < -200$ nT) are caused by fast CMEs moving at speeds higher than 1500 km s^{-1}. The converse, however, may not always be true.

[31] 6. The travel time of a CME shows a strong dependence on its initial speed. The CME with high speeds greater than 1500 km s^{-1} arrive in ∼30 ± 5 hours at the Earth and trigger the onset of the geomagnetic storm. For the CMEs that have lower initial speeds in the range of 500–1000 km s^{-1}, the travel time has an average value of ∼80 hours, which is consistent with the average value for the solar minimum period [*Brueckner et al.*, 1998]. From our data set we found that the relation between the arrival time (marked by the onset of the geomagnetic storm) and the initial speed is given by $T = 86.9 - 0.026\ V$.

[32] 7. An interplanetary shock is a good indicator of arrival of ejecta at the Earth; the shock speed, however, does not appear to be a very reliable predictor for the resulting storm intensity.

[33] 8. An early-on prediction of the strength or the magnitude of geomagnetic storms depends on the prediction of the ram pressure because a high ram pressure leads to the compression of the magnetic cloud and intensifies the southward component of B_z. The knowledge of projected initial speed of the CMEs can be used to predict the ram pressure early on but with low levels of confidence. Our analysis shows that one requires additional information on the density of the CME and its variation through the IP medium for a better prediction of the ram pressure, which in turn can be used to predict the strength of the resulting storm with less uncertainty.

[34] To summarize, the study shows that the fast full halo CMEs associated with strong flares and originating from a favorable location, i.e., close to the central meridian and low and middle latitudes, are the most potential candidates for producing strong ram pressure

at the Earth's magnetosphere and hence intense geomagnetic storms. We used the solar, interplanetary, and geomagnetic data for 64 events recorded during the 1996–2002 to compute correlation coefficients between important solar, interplanetary, and geomagnetic activity parameters. These investigations reveal that the intensity of geomagnetic storms depends most strongly on the southward component of the interplanetary magnetic field, followed by the initial speed and ram pressure of the geoeffective CME. The strength of the resulting storm can be predicted with some confidence, if the ram pressure can be predicted early on from the initial speed and density of a geoeffective CME. Therefore it is important to measure the initial speeds and densities of geoeffective CMEs with high accuracy for predicting the intensity of the resulting geomagnetic storm. Most of the existing prediction schemes are largely based on the inputs from the interplanetary sources of the storms and are drawn from the original formula of *Burton et al.* [1975] [e.g., *Feldstein*, 1992; *Fenrich and Luhmann*, 1998; *O'Brien and McPherron*, 2000]. Our results can prove very useful in developing a new scheme for predicting the intensity of a geomagnetic storm from solar origins.

References

Bothmer, V., and R. Schwenn (1995), Eruptive prominences as sources of magnetic clouds in the solar wind, *Space Sci. Rev.*, *70*, 215.

Brueckner, G. E., et al. (1995), The Large Angle Spectroscopic Coronagraph (LASCO), *Solar Phys.*, *162*, 357.

Brueckner, G. E., et al. (1998), Geomagnetic storms caused by coronal mass ejections (CMEs): March 1996 through June 1997, *Geophys. Res. Lett.*, *25*, 3019.

Burton, R. K., R. L. McPherron, and C. T. Russell (1975), An empirical relationship between interplanetary conditions and D_{ST}, *J. Geophys. Res.*, *80*, 4204.

Cane, H. V., I. G. Richardson, and O. C. St. Cyr (2000), Coronal mass ejections, interplanetary ejecta, and geomagnetic storms, *Geophys. Res. Lett.*, *27*, 3591.

Crooker, N. U., and A. H. McAllister (1997), Transients associated with recurrent storms, *J. Geophys. Res.*, *102*, 14,041.

Delaboudiniere, J.-P., et al. (1995), Extreme Ultraviolet Imaging telescope for the SoHO mission, *Solar Phys.*, *162*, 291.

Domingo, V., B. Fleck, and A. I. Poland (1995), The SOHO Mission: An overview, *Solar Phys.*, *162*, 1.

Feldstein, Y. I. (1992), Modelling of the magnetic field, *Space Sci. Rev.*, *59*, 83.

Fenrich, F. R., and J. G. Luhmann (1998), Geomagnetic response to magnetic clouds of different polarity, *Geophys. Res. Lett.*, *25*, 2999.

Feynman, J., and S. B. Gabriel (2000), On space weather consequences and predictions, *J. Geophys. Res.*, *105*, 10,543.

Gonzalez, W. D., B. T. Tsurutani, A. L. C. Gonzalez, E. J. Smith, F. Tang, and S. Akasofu (1989), Solar wind-magnetospsheic coupling during intense magnetic storms, *J. Geophys. Res.*, *94*, 8835.

Gonzalez, W. D., A. L. C. Gonzalez, and B. T. Tsurutani (1990), Dual-peak solar cycle distribution of intense geomagnetic storms, *Planet. Space Sci.*, *38*, 181.

Gonzalez, W. D., B. T. Tsurutani, P. S. McIntosh, and A. L. C. Gonzalez (1996), Coronal holes-active regions-current sheet association with intense interplanetary and geomagnetic phenomena, *Geophys. Res. Lett.*, *23*, 2577.

Gonzalez, W. D., A. L. C. Gonzalez, A. Dal Lago, B. T. Tsurutani, J. K. Arballo, G. S. Lakhina, B. Buti, C. M. Ho, and S.-T. Wu (1998), Mag-

netic cloud field intensities and solar wind velocities, *Geophys. Res. Lett.*, *25*, 963.

Gonzalez, W. D., B. T. Tsurutani, and A. L. C. Gonzalez (1999), Interplanetary origin of geomagnetic storms, *Space Sci. Rev.*, *88*, 529.

Gopalswamy, N., A. Lara, R. P. Lepping, M. L. Kaiser, D. Berdichevsky, and O. C. St. Cyr (2000), Interplanetary acceleration of coronal mass ejections, *Geophys. Res. Lett.*, *27*, 145.

Gopalswamy, N., A. Lara, S. Yashiro, M. L. Kaiser, and R. A. Howard (2001a), Predicting the 1-AU arrival times of coronal mass ejections, *J. Geophys. Res.*, *106*, 29,207.

Gopalswamy, N., A. Lara, M. L. Kaiser, and J.-L. Bougeret (2001b), Near-Sun and near-Earth manifestation of solar eruptions, *J. Geophys. Res.*, *106*, 25,261.

Gosling, J. T. (1993a), Coronal mass ejection—The link between solar and geomagnetic activity, *Phys. Fluids*, *5*, 2639.

Gosling, J. T. (1993b), The solar flare myth, *J. Geophys. Res.*, *98*, 18,937.

Gosling, J. T., S. J. Bame, D. J. McComas, and J. L. Phillips (1990), Coronal mass ejections and large geomagnetic storms, *Geophys. Res. Lett.*, *17*, 901–904.

Gosling, J. T., D. J. McComas, J. L. Philips, and S. J. Bame (1991), Geomagnetic activity associated with earth passage of IP shock disturbances and coronal mass ejections, *J. Geophys. Res.*, *96*, 731.

Hovestadt, D., et al. (1995), CELIAS Charge Element and Isotope analysis system for SoHO, *Solar Phys.*, *162*, 441.

Howard, R. A., D. J. Michels, N. R. Sheeley Jr., and M. J. Koomen (1982), The observation of a coronal transient directed at the earth, *Astrophys. J. Lett.*, *263*, L101.

Hundhausen, A. J. (1972), *Coronal Expansion and Solar Wind*, p. 174, Springer-Verlag, New York.

Hundhausen, A. J. (1997), Coronal mass ejections, in *Cosmic Winds and the Heliosphere*, edited by J. R. Jokipii, C. P. Sonett, and M. S. Giampapa, p. 259, Univ. of Arizona Press, Tucson, Ariz.

Kahler, S. (1977), The morphological and statistical properties of solar X-ray events with long decay times, *Astrophys. J.*, *214*, 891.

Kamide, Y., et al. (1998), Current understanding of magnetic storms: Storm-substorm relationships, *J. Geophys. Res.*, *103*, 17,705.

Lindsay, G. M., C. T. Russell, and J. G. Luhmann (1995), Coronal mass ejection and stream interaction region characteristics and their potential geomagnetic effectiveness, *J. Geophys. Res.*, *100*, 16,999.

Luhmann, J. (1997), What do we really know about solar-wind coupling, *Adv. Space Res.*, *20*, 907.

O'Brien, T. P., and R. L. McPherron (2000), An empirical phase space analysis of ring current dynamics: Solar wind control of injection and decay, *J. Geophys. Res.*, *105*, 7707.

Plunkett, S. P., et al. (2001), Source regions of coronal mass ejections and their geomagnetic effects, *J. Atmos. Sol. Terr. Phys.*, *63*, 38.

Richardson, I. G., E. W. Cliver, and H. V. Cane (2000), Sources of geomagnetic storms over the solar cycle: Relative importance of coronal mass ejections, high-speed streams, and slow solar wind, *J. Geophys. Res.*, *105*, 18,203.

Richardson, I. G., E. W. Cliver, and H. V. Cane (2001), Sources of geomagnetic storms for solar minimum and maximum conditions during 1972–2000, *Geophys. Res. Lett.*, *28*, 2569.

Richardson, I. G., H. V. Cane, and E. W. Cliver (2002), Sources of geomagnetic activity during nearly three solar cycles (1972–2000), *J. Geophys. Res.*, *107*(A8), 1187, doi:10.1029/2001JA000504.

Shea, M. A., and D. F. Smart (1996), Solar proton fluxes as a function of the observation location with respect to the parent solar activity, *Adv. Space Res.*, *17*, 4–5.

Sheeley, N. R., Jr., et al. (1975), Coronal changes associated with a disappearing filament, *Solar Phys.*, *45*, 377.

Srivastava, N., and P. Venkatakrishnan (2002), Relation between CME speed and geomagnetic storm intensity, *Geophys. Res. Lett.*, *29*(9), 1287, doi:10.1029/2001GL013597.

Srivastava, N., W. D. Gonzalez, A. L. C. Gonzalez, and S. Masuda (1997), On the characteristics of solar origins of geo-effective CMEs observed during August 1992–April 1993, in *Correlated Phenomena at the Sun, in the Heliosphere, and in Geospace*, ESA Publ. SP-415, p. 443, Eur. Space Agency, Paris.

Srivastava, N., W. D. Gonzalez, A. L. C. Gonzalez, and S. Masuda (1998), On the solar origins of intense geomagnetic storms observed during 6–11 March 1993, *Solar Phys.*, *183*, 419.

St. Cyr, O. C., et al. (2000), Properties of coronal mass ejections: SOHO LASCO observations from January 1996 to June 1998, *J. Geophys. Res.*, *105*, 18,169.

Stone, E. C., A. M. Frandsen, R. A. Mewaldt, E. R. Christian, D. Margolies, J. F. Ormes, and F. Snow (1998), The Advanced Composition Explorer, *Space Sci. Rev.*, *86*, 1.

Thompson, B. J., et al. (1998), SOHO/EIT Observations of an Earth-directed coronal mass ejection on May 12, 1997, *Geophys. Res. Lett.*, *25*, 2465.

Tsurutani, B. T. and W. D. Gonzalez (1997), The interplanetary causes of magnetic storms: A review, in *Magnetic Storms*, Geophys. Monogr. Ser., vol. 98, edited by B. T. Tsurutani, W. D. Gonzalez, and Y. Kamide, p. 77, AGU, Washington, D. C.

Tsurutani, B. T., W. D. Gonzalez, F. Tang, S. I. Akasofu, and E. J. Smith (1988), Solar wind southward Bz features responsible for major magnetic storms of 1978–1979, *J. Geophys. Res.*, *93*, 8519.

Tsurutani, B. T., B. E. Goldstein, E. J. Smith, W. D. Gonzalez, F. Tang, S. I. Akasofu, and R. R. Anderson (1990), The interplanetary and solar causes of geomagnetic activity, *Planet. Space Sci.*, *38*, 109.

Venkatakrishnan, P., and B. Ravindra (2003), Relationship between CME speeds and magnetic energy of active regions, *Geophys. Res. Lett.*, *30*(23), 2181, doi:10.1029/2003GL018100.

Wang, Y. M., P. Z. Ye, S. Wang, G. P. Zhou, and J. X. Wang (2002), A statistical study on the geoeffectiveness of Earth-directed coronal mass ejections from March 1997 to December 2000, *J. Geophys. Res.*, *107*(A11), 1340, doi:10.1029/2002JA009244.

Webb, D. F. (1992), The solar sources of coronal mass ejections, in *Eruptive Solar Flares, Proceedings of IAU Colloquium 133*, edited by Z. Svestka, B. V. Jackson, and M. E. Machado, p. 234, Springer-Verlag, New York.

Webb, D. F., and A. J. Hundhausen (1987), Activity associated with the solar origin of coronal mass ejections, *Solar Phys.*, *108*, 383.

Webb, D. F., and B. V. Jackson (1990), The identification and characteristics of solar mass ejections observed in the heliosphere by the Helios-2 photometers, *J. Geophys. Res.*, *95*, 20,641.

Webb, D. F., S. W. Kahler, P. S. McIntosh, and J. A. Klimchuk (1997), Large-scale structures and multiple neutral lines associated with coronal mass ejections, *J. Geophys. Res.*, *102*, 24,161.

Webb, D. F., E. W. Cliver, N. Crooker, O. C. St. Cyr, and B. J. Thompson (2000), The relationship of halo CMEs, magnetic clouds and geomagnetic storms, *J. Geophys. Res.*, *105*, 7491.

Zhang, J., K. P. Dere, R. A. Howard, and V. Bothmer (2003), Identification of solar sources of major geomagnetic storms between 1996 and 2000, *Astrophys. J.*, *582*, 520.

————————————

N. Srivastava and P. Venkatakrishnan, Udaipur Solar Observatory, P.O. Box 198, Badi Road, Dewali, Udaipur 313001, India. (nandita@prl.ernet.in)